A novel mechanism for the oxidation reaction of VO^{2+} on a graphite electrode in acidic solutions

Wenjun Wang, Xinzhuang Fan*, Jianguo Liu, Chuanwei Yan, Chaoliu Zeng*

State Key Laboratory for Corrosion and Protection, Institute of Metal Research, Chinese Academy of Sciences, 62 Wencui Road, Shenyang 110016, China

HIGHLIGHTS

- The reaction orders of VO^{2+} and H^+ for the oxidation reaction of VO^{2+} are calculated.
- A new reaction mechanism is proposed to describe the oxidation of VO^{2+}.
- A real kinetic equation is built up for the oxidation reaction of VO^{2+}.

ARTICLE INFO

ABSTRACT

With the consideration of optimizing the performance of the all-vanadium redox flow battery (VRB), the oxidation reaction mechanism of VO^{2+} on a rotating graphite disk electrode has been investigated by potentiodynamic polarization in sulfuric acid solutions with various *pH* and vanadium concentrations. Furthermore, the reaction orders of VO^{2+} and H^+ for the oxidation reaction of VO^{2+} have been calculated from the polarization results and compared with the theoretical results according to the possible reaction mechanisms available in the literature. However, a new oxidation reaction mechanism has been proposed to describe the oxidation of VO^{2+} at last, and the theoretic reaction orders of VO^{2+} and H^+ based on the new mechanism are consistent with the experimental results when the electrochemical reaction is the rate-limited process. Moreover, a corresponding kinetic equation has been established for the oxidation reaction of VO^{2+} on a spectroscopically pure graphite electrode, and can be well used to predict the polarization behavior in V (IV) acidic solutions.

© 2014 Elsevier B.V. All rights reserved.

1. Introduction

With the rapid and continuous exhaustion of the available fossil fuel, the renewable energy resources such as wind, solar and tidal power are required to be efficiently developed and utilized in future. Due to the random and intermittent nature of these renewable energy resources, energy storage technologies should be obtained for their stabilization and smooth output [1]. To date, as an electrochemical energy storage system the all-vanadium redox flow battery (VRB) using the same element in both half-cells has shown a great promise in various pre- commercial to commercial stationary applications [2], with some attractive features like quick charging-discharging, simple structure, flexible design, high efficiency, high safety and long cycle life [3]. In the VRB, the VO_2^+/VO^{2+} and V^{2+}/V^{3+} couples in concentrated sulfuric acid solutions are

applied as positive and negative electrolytes, respectively. VRB releases or stores the electric energy through the valence-state changes of vanadium ions, involving the migration of vanadium ions in the electrolytes and the oxidation or reduction process of vanadium ions at the electrodes. Thereby, it is of great significance to understand the kinetic processes of redox reactions at the electrodes of VRB for developing electrode materials and optimizing the VRB structure.

In comparison with the negative V^{2+}/V^{3+} couple, the redox reaction for the positive VO_2^+/VO^{2+} couple is more complicated, with a multistep reaction process involving an oxygen transfer reaction before or after an electron-transfer step [1]. Since the concept of VRB was proposed by Skyllas-Kazacos et al. in the 1980s [4,5], only a limited number of investigations on the redox reaction mechanism of the VO_2^+/VO^{2+} couple have been available [6–11]. In a study of the redox reaction mechanism of the VO_2^+/VO^{2+} couple at a rotating disk graphite electrode in acidic aqueous solutions, Gattrell et al. [6] observed unusually high Tafel slopes for the reduction of V (V), and suggested that the oxidation reaction of VO^{2+} follows a

multistep electrochemical-chemical-chemical (ECC) mechanism, while the reduction reaction mechanism of VO_2^+ changes from a multistep chemical-electrochemical-chemical (CEC) mechanism at low cathodic overpotentials to a multistep electrochemical-chemical-chemical (ECC) mechanism at high cathodic overpotentials. However, the unusually high Tafel slopes (350–450 mV decade^{-1}) observed for the reduction of VO_2^+ at higher overpotentials could not be well explained by the model. To understand the unusual Tafel slope, Gattrel et al. [7] further investigated the electrochemical reduction of VO_2^+ at high overpotentials by polarization and double layer measurements, and established a model involving electron transfer through an adsorbed layer of vanadium species to explain the change of the reduction reaction mechanism of VO_2^+ [7]. The experimental data for the redox reactions of the VO_2^+/VO^{2+} couple on a rotating graphite disk electrode have fitted well with the computational simulation results based on the above model to some extent [6,7]. Additionally, Oriji et al. [11] reported that the redox processes of the VO_2^+/VO^{2+} couple at a carbon plate electrode in both directions are not simple and a probable reversible chemical step with the breaking/formation of the V–O chemical bond follows an electron transfer step of the VO_2^+/VO^{2+} reaction in a V (IV) or V (V) solution. Thereby, more investigations are still required to understand the mechanism and kinetic processes of the redox reactions of the VO_2^+/VO^{2+} couple on carbon electrodes.

In this paper, the oxidation reaction of VO^{2+} has been investigated by steady-state potentiodynamic polarization on rotating graphite and glassy carbon disk electrodes in sulfuric acid solutions with various *pH* and vanadium concentrations in an attempt to establish its reaction mechanism.

2. Experimental

2.1. Preparation and chemical analysis of electrolyte solutions

All chemicals used in the present experiments were analytically pure agents and all solutions were prepared with de-ionized water. V (IV) acidic solutions were produced by dissolving $VOSO_4 \cdot nH_2O$ ($n = 2.82$, according to the chemical precipitation method) in sulfuric acid solutions and then diluted to produce the solutions with various *pH* and vanadium concentrations. In addition, the measurements of *pH* and viscosity of the electrolytes were performed with a pHS-25 *pH* meter (Shanghai Precision Instrument Co. Ltd, China) and a NDJ-5S digital torsion viscosimeter (Shanghai Ni Run Intelligent Technology Co. Ltd, China), respectively.

2.2. Electrochemical measurements

Electrochemical measurements were undertook with a rotating disk system (Pine Instruments) including basal plane pyrolytic graphite (GB) and glassy carbon (GC) disc electrodes (0.196 cm^2), an AFMSRCE electrode rotator, an AFE6MB shaft and a cell, with a platinum plate as the counter electrode and a saturated calomel electrode (SCE) as the reference electrode. A salt bridge was used to eliminate the liquid junction potential between the Luggin capillary and working electrode. The electrodes attached to the rotating disk system were initially polished with aqueous slurries with alumina powders (average particle diameter: 0.6 μm) on a piece of chamois cloth and then ultrasonically cleaned for 5 min in alcohol and de-ionized water in turn. Steady-state polarization curves at the scan rate of 1 mV s^{-1} were obtained with the rotating disk system at room temperature in V (IV) acidic solutions. All the electrochemical measurements were performed by a CHI730C Electrochemical Analysis

Instrument (Shanghai Chenhua Instrument Co. Ltd, China). Additionally, some potentiodynamic polarization curves were also obtained on a spectroscopically pure graphite electrode (0.283 cm^2, Sinosteel Shanghai Advanced Graphite Material Co. Ltd, China) at the scan rate of 0.5 mV s^{-1} in static V (IV) acidic solutions at various temperatures controlled with a water bath. The electrode was ground with down to 2000 grit silicon carbide papers, followed by polishing with a flanelle and thoroughly rinsing with alcohol before use.

3. Results and discussion

3.1. Effect of rotation rate

Fig. 1 shows the polarization curves of the rotating pyrolytic graphite disk electrode at various rotation rates in 0.5 M $VOSO_4$ + 3.0 M H_2SO_4 solution. The limiting diffusion current (I_d) increases with the increase of rotation rate, due to the fact that a higher rotation rate contributes a thinner diffusion layer [12]. However, the anodic oxidation current changes little when the rotation rate is higher than 1600 rpm, suggesting that a rotation rate larger than 1600 rpm is favorable to study the oxidation reaction mechanism of VO^{2+}. Thus, a rotation rate of 2000 rpm has been selected for the subsequent measurements on the rotating disk electrode (RDE).

3.2. Reaction order measurements

3.2.1. Reaction order of VO^{2+}

Fig. 2a gives the polarization curves of the pyrolytic graphite electrode at the rotating rate of 2000 rpm in $VOSO_4$ + 3.0 M H_2SO_4 solutions containing various concentrations of VO^{2+}. Fig. 2b shows clearly that the shift of the polarization potential (E) with the logarithmic current (lg$I$) follows a linear law at potentials from 0.90 to 1.02 V, suggesting that the oxidation reaction of VO^{2+} is controlled by the electrochemical polarization. The reaction order of VO^{2+} ($m_{VO^{2+}}$) can be calculated at a certain potential by the following equation [13]:

$$m = \left(\frac{\partial \lg I}{\partial \lg C_{VO^{2+}}} \right)_E \tag{1}$$

where I is the anodic current at a certain potential (E), $C_{VO^{2+}}$ is the bulk concentration of VO^{2+}.

From Fig. 2a and b, the plots of lg$I$ vs. lg$C_{VO^{2+}}$ at different potentials are obtained, as shown in Fig. 2c. The change of lg$I$ with
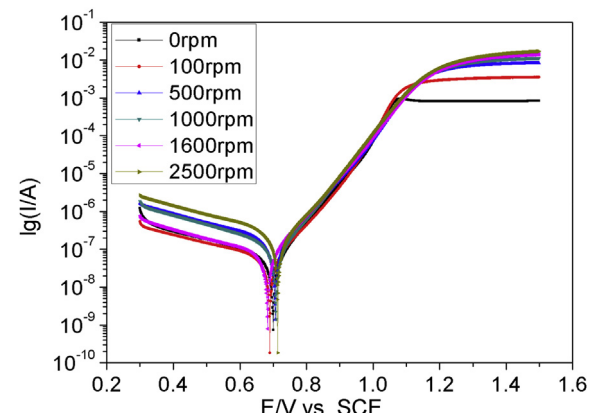

Fig. 1. Polarization curves at various rotating rates on the pyrolytic graphite electrode with the sweep rate of 1 mV s^{-1} in 0.5 M $VOSO_4$ + 3.0 M H_2SO_4 solution.
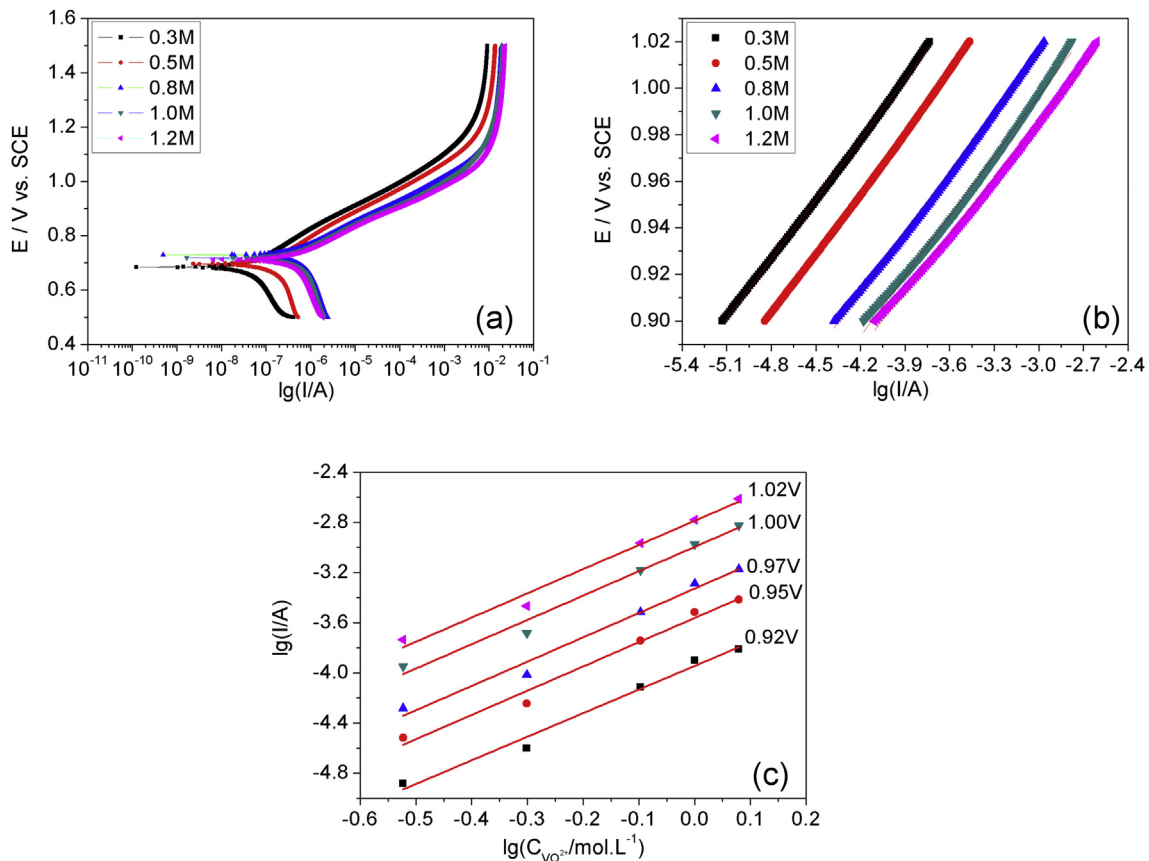
Fig. 2. Polarization curves (a, b) at varying concentrations of VO^{2+} and the corresponding logarithmic current as a function of the logarithmic concentration of VO^{2+} at various electrode potentials (c) on the pyrolytic graphite electrode at the rotating rate of 2000 rpm with the sweep rate of 1 mV s^{-1} in VOSO$_4$ + 3.0 M H$_2$SO$_4$ solution.

lgC$_{VO^{2+}}$ is approximately linear, and thus the values of $m_{VO^{2+}}$ (the slope of the plots) at various potentials are estimated, as seen in Table 1. The mean value of $m_{VO^{2+}}$ is 1.92 for the oxidation reaction of VO^{2+} on the pyrolytic graphite electrode.

Fig. 3a and b present the polarization curves of the rotating glassy carbon disk electrode with a rotating rate of 2000 rpm in VOSO$_4$+ 3.0 M H$_2$SO$_4$ solutions containing various concentrations of VO^{2+} and the corresponding plots of lgI vs. lgC$_{VO^{2+}}$ at different potentials, respectively. Linear Tafel regions appear distinctly on the polarization curves. However, some non-linear features are also observed on the polarization curves at high overpotentials more than 120 mV, probably due to the glassy carbon electrode with a low activation. Therefore, linear Tafel regions at as high overpotentials as possible are selected to calculate the reaction orders. The mean reaction order of VO^{2+} ($m_{VO^{2+}}$) is similarly calculated to be 1.55, as listed in Table 2. Based on the above results, it is approximately thought that the oxidation reaction order of VO^{2+} on carbon electrodes is 2. It should also be noted that as compared to the pyrolytic graphite electrode (Fig. 2a), the open circuit potential for the glassy carbon electrode shifts negatively by around 300 mV, except for the solution containing 0.5 M VO^{2+}. This may be ascribed to their differences in the structure and surface activation.

3.2.2. Reaction order of H$^+$

Fig. 4a presents the polarization curves for the rotating pyrolytic graphite electrode in 0.5 M VOSO$_4$ + H$_2$SO$_4$ solutions with various values of pH. At the potentials from 0.75 to 0.9 V, E is linearly proportional to lgI (Fig. 4b), suggesting that the electrochemical polarization is a rate determining process for the oxidation reaction of VO^{2+}. The reaction order of H$^+$ (m_{H^+}) can be estimated as the following equation [13]:

$$m = \left(-\frac{\partial \lg I}{pH} \right)_E \tag{2}$$

Fig. 4c gives the shift of lgI with pH at various potentials. The values of m_{H^+} can be obtained from the slope of the plots in Fig. 4c, as listed in Table 3. The average value of m_{H^+} is −1.03 for the oxidation reaction of VO^{2+} on the pyrolytic graphite electrode. Similarly, the reaction order of H$^+$ on the rotating glassy carbon electrode has also been investigated, as shown in Fig. 5 and Table 4, respectively. Additionally, some non-linear features on the polarization curves are similarly observed in Fig. 5a. The average value of m_{H^+} is −0.89. As a result, the value of m_{H^+} can be considered as −1 for the oxidation reaction of VO^{2+} on carbon electrodes.

3.3. Theoretical calculations of reaction order

The above results indicate that the reaction order of VO^{2+} and H$^+$ for the oxidation of VO^{2+} on carbon electrodes is 2 and −1, respectively. The confirmation of these reaction orders is helpful for understanding the oxidation reaction process of VO^{2+}. Before establishing the reaction mechanism of VO^{2+}, it is necessary to

Table 1
The reaction order of VO^{2+} during the oxidation reaction of VO^{2+} on the pyrolytic graphite electrode.

E/V	0.92	0.95	0.97	1.00	1.02	Mean value of $m_{VO^{2+}}$
$m_{VO^{2+}}$	1.88	1.93	1.94	1.94	1.93	1.92

discuss theoretically the reaction models available. Gattrell et al. [6] have proposed that the oxidation reaction of VO^{2+} is likely to follow a three-step reaction mechanism such as chemical (C)-chemical (C)-electrochemical (E), ECC and CEC mechanism. In addition, Oriji et al. [11] have also suggested that the electron transfer step (E step) is followed by a certain chemical step (C step) for the oxidation reaction of VO^{2+}. Thereby, in the following discussions ECC and CEC mechanisms will be considered.

3.3.1. Calculations based on an ECC mechanism

Supposing the oxidation reaction of VO^{2+} is consistent with an ECC mechanism, then the electrochemical and chemical steps are expressed as follows [6]:

$$VO^{2+} \cdot 5H_2O \underset{k_{-3}}{\overset{k_3}{\rightleftharpoons}} VO^{3+} \cdot 5H_2O + e \tag{3}$$

$$VO^{3+} \cdot 5H_2O \underset{k_{-4}}{\overset{k_4}{\rightleftharpoons}} VO_2^+ \cdot 4H_2O + 2H^+ \tag{4}$$
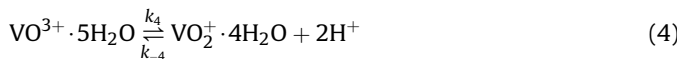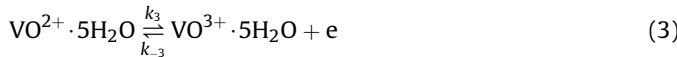
In the present calculations, two chemical steps are combined to be one chemical step of step (4). Any reaction rate constants (k) are considered to be unconcerned with the electrode potential (E) in this paper, except for special annotations.

If step (3) is rate determining, the reaction current density i is given by:

$$i = Fk_3 \left[VO^{2+}\right] \exp\left[\frac{\beta}{RT}FE\right] \tag{5}$$

where k_3 is the forward reaction rate constant of step (3), $[VO^{2+}]$ represents the bulk concentration of VO^{2+}, β is the anodic charge transfer coefficient, E is the electrode potential, the other symbols such as F, R and T have their usual meanings.

Then the reaction orders of VO^{2+} ($m_{VO^{2+}}$) and H^+ (m_{H^+}) can be obtained from eq. (5) as follows:

$$m_{VO^{2+}} = \frac{\partial \lg i}{\partial \lg \left[VO^{2+}\right]} = 1 \tag{6}$$

$$m_{H^+} = \frac{\partial \lg i}{\partial \lg \left[H^+\right]} = 0 \tag{7}$$

On the other hand, assuming that step (4) is rate determining and step (3) is close to equilibrium, the reaction current density i is defined as:
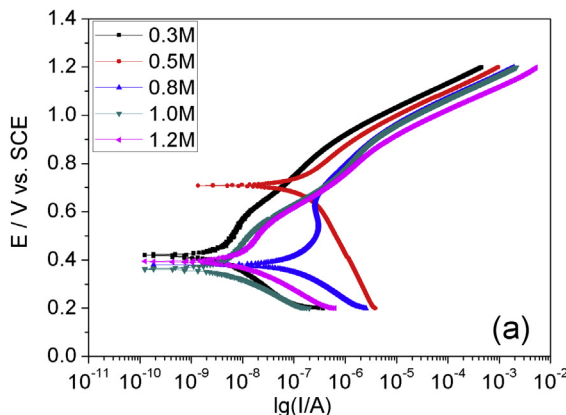
Table 2
The reaction order of VO^{2+} during the oxidation reaction of VO^{2+} on the glassy carbon electrode.

E/V	0.87	0.9	0.92	0.95	0.97	Mean value of $m_{VO^{2+}}$
$m_{VO^{2+}}$	1.57	1.55	1.55	1.55	1.55	1.55

$$i = Fk_4 \left[VO^{3+}\right] \tag{8}$$

when step (3) is at equilibrium, the same reaction rate in both directions is described by:

$$k_3 \left[VO^{2+}\right] \exp\left[\frac{\beta}{RT}FE\right] = k_{-3} \left[VO^{3+}\right] \exp\left[\frac{-(1-\beta)}{RT}FE\right] \tag{9}$$

where k_{-3} is the reverse reaction rate constant of step (3).

According to eqs. (8) and (9), the reaction current density i can be expressed by eqn. (10):

$$i = F\frac{k_4 k_3}{k_{-3}} \left[VO^{2+}\right] \exp\left[\frac{FE}{RT}\right] \tag{10}$$

Thus, the values of $m_{VO^{2+}}$ and m_{H^+} can be calculated as:

$$m_{VO^{2+}} = \frac{\partial \lg i}{\partial \lg \left[VO^{2+}\right]} = 1 \tag{11}$$

$$m_{H^+} = \frac{\partial \lg i}{\partial \lg \left[H^+\right]} = 0 \tag{12}$$

The above calculations indicate that in case the oxidation reaction of VO^{2+} follows an ECC mechanism, the reaction order of VO^{2+} and H^+ is 1 and 0, respectively. It is clear that the theoretical reaction orders are inconsistent with the experimental results, suggesting that the oxidation of VO^{2+} may follow a different mechanism.

3.3.2. Calculations based on a CEC mechanism

According to a CEC mechanism, the oxidation reaction of VO^{2+} is as follows [6]:

$$VO^{2+} \cdot 5H_2O \underset{k_{-13}}{\overset{k_{13}}{\rightleftharpoons}} HVO_2^+ \cdot 4H_2O + 2H^+ \tag{13}$$

$$HVO_2^+ \cdot 4H_2O \underset{k_{-14}}{\overset{k_{14}}{\rightleftharpoons}} HVO_2^{2+} \cdot 4H_2O + e \tag{14}$$
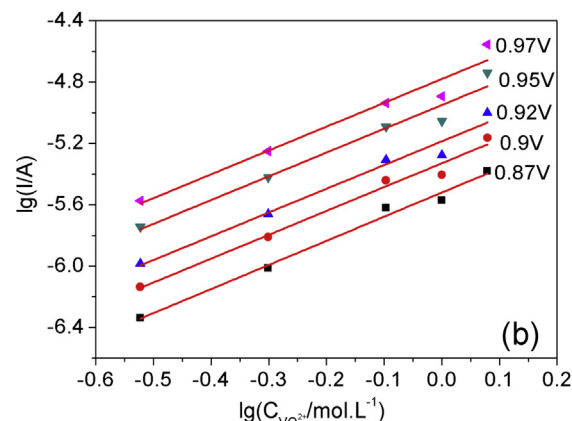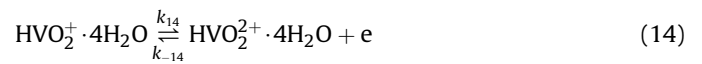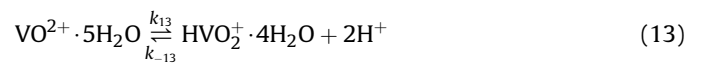
Fig. 3. Polarization curves at various concentrations of VO^{2+} (a) and the logarithmic current as a function of the logarithmic concentration of VO^{2+} at various electrode potentials (b) on the glassy carbon electrode at 2000 rpm with the sweep rate of 1 mV s^{-1} in VOSO$_4$ + 3.0 M H$_2$SO$_4$ solution.

$$HVO_2^{2+} \cdot 4H_2O \underset{k_{-15}}{\overset{k_{15}}{\rightleftharpoons}} VO_2^+ \cdot 4H_2O + H^+ \tag{15}$$
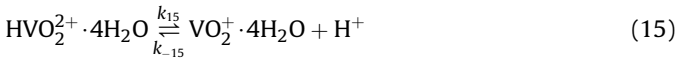
Firstly, assuming that step (13) is rate determining, the reaction current density is illustrated as:

$$i = Fk_{13}\left[VO^{2+}\right] \tag{16}$$

Then, the values of $m_{VO^{2+}}$ and m_{H^+} are calculated to be 1 and 0, respectively.

Secondly, if step (14) is rate determining and the other steps are close to equilibrium, the reaction current density is given by:

$$i = Fk_{14}\left[HVO_2^+\right]\exp\left[\frac{\beta}{RT}FE\right] \tag{17}$$

Because step (13) is at equilibrium, the forward reaction rate is equal to the reverse one:

$$k_{13}\left[VO^{2+}\right] = k_{-13}\left[H^+\right]\left[HVO_2^+\right] \tag{18}$$

According to eqs. (17) and (18), the reaction current density is expressed by:

$$i = Fk_{14}\frac{k_{13}\left[VO^{2+}\right]}{k_{-13}\left[H^+\right]}\exp\left[\frac{\beta}{RT}FE\right] \tag{19}$$

From eq. (19) the values of $m_{VO^{2+}}$ and m_{H^+} are calculated to be 1 and −1, respectively.

Finally, if the reaction (15) is rate determining, then the reactions (13) and (14) can be approximately considered to be at equilibrium. The reaction current density is shown as:
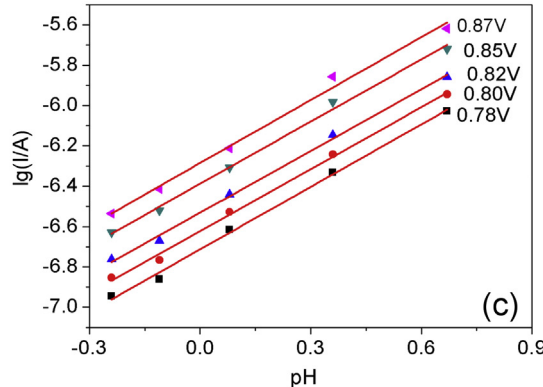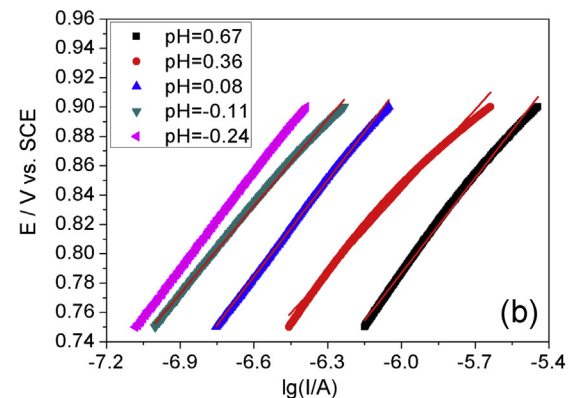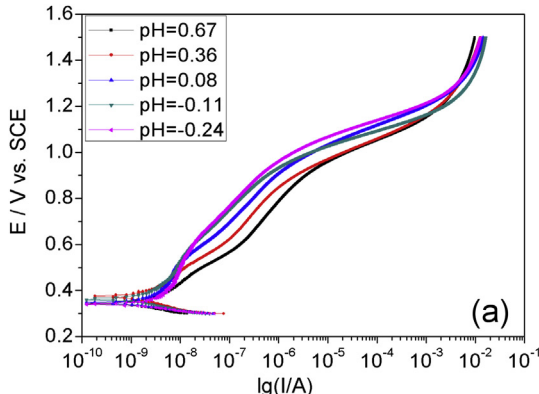
Table 3
The reaction order of H^+ on the pyrolytic graphite electrode during the oxidation reaction of VO^{2+}.

E/V	0.78 V	0.8 V	0.82 V	0.85 V	0.87 V	Mean value of m_{H^+}
m_{H^+}	−1.03	−1.02	−1.02	−1.03	−1.04	−1.03

$$i = Fk_{15}\left[HVO_2^{2+}\right] \tag{20}$$

The following expressions are obtained for the reactions (13) and (14) at equilibrium:

$$Fk_{14}\left[HVO_2^+\right]\exp\left[\frac{\beta}{RT}FE\right] = Fk_{-14}\left[HVO_2^{2+}\right]\exp\left[\frac{-(1-\beta)}{RT}FE\right] \tag{21}$$

Thus, according to eqs. (18), (20) and (21), the reaction current density is presented as below:

$$i = F\frac{k_{15}k_{14}k_{13}}{k_{-14}k_{-13}}\frac{\left[VO^{2+}\right]}{\left[H^+\right]}\exp\left[\frac{FE}{RT}\right] \tag{22}$$

It can be estimated from eq. (22) that the values of $m_{VO^{2+}}$ and m_{H^+} are 1 and −1, respectively.

The above calculations show that if the oxidation of VO^{2+} follows the CEC mechanism the theoretic values of $m_{VO^{2+}}$ and m_{H^+} are different from the experimental results, suggesting that the oxidation reaction of VO^{2+} does not obey the CEC mechanism as well.

Fig. 4. Polarization curves (a, b) at varying pH and lg*I* as a function of pH at various electrode potentials (c) on the pyrolytic graphite electrode at 2000 rpm with the sweep rate of 1 mV s^{-1} in 0.5 M VOSO$_4$ + H$_2$SO$_4$ solution.
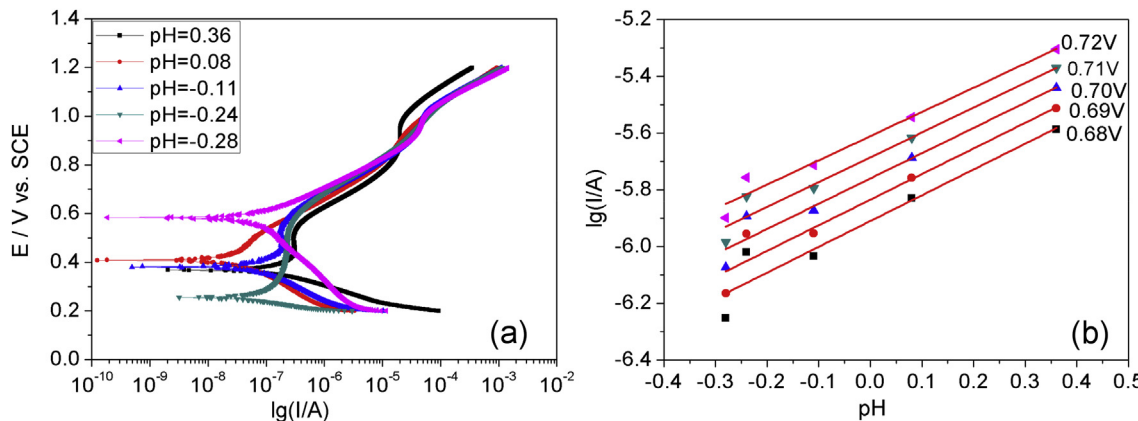
Fig. 5. Polarization curves at varying *pH* (a) and the plot of lg*I* vs. *pH* at various electrode potentials (b) on the glassy carbon electrode at 2000 rpm with the sweep rate of 1 mV s^{-1} in 0.5 M VOSO$_4$ + H$_2$SO$_4$ solution.

3.4. A new consideration for the oxidation mechanism of VO^{2+}

The above experimental results suggest that the reaction order of VO^{2+} and H$^+$ for the oxidation of VO^{2+} on carbon electrodes is 2 and -1, respectively. To understand the reaction mechanism it is necessary to know the electron transfer number (n) of the oxidation reaction of VO^{2+}. From Fig. 1, the shift of I_d at the potential of 1.4 V with the square root of the rotation rate ($\omega^{1/2}$) was obtained, as shown in Fig. 6. Fig. 6 shows clearly that the change I_d vs. $\omega^{1/2}$ is approximately linear. The value of n can be determined from the slope of the plot by Levich's equation [12]:

$$I_d = 0.62nFAD_{VO^{2+}}^{2/3}\nu^{-1/6}\omega^{1/2}C_{VO^{2+}} \quad (23)$$

where A is the area of the electrode, $D_{VO^{2+}}$ the diffusion coefficient of VO^{2+}, ν the kinematic viscosity of the electrolyte and $C_{VO^{2+}}$ the bulk concentration of VO^{2+}.

ν can be defined by the following equation [14]:

$$\eta = \nu \times \rho \quad (24)$$

where η is the kinetic viscosity of the electrolyte and ρ is the density of the solution.

For the present system, the values of $D_{VO^{2+}}$ and ρ can be assumed as 10^{-6} cm^{-2} s^{-1} [11] and 1.2 g cm^{-3} [14], respectively. The kinetic viscosity of the electrolyte (η) is measured as 2.85 mPa s. Thus, the value of n is estimated as 0.81 from eqs. (23) and (24). It can be deduced that the electron transfer number (n) of the oxidation reaction of VO^{2+} is approximately 1. It has been accepted that in acidic solutions with a H$_2$SO$_4$ concentration less than 4.0 M, VO^{2+} and VO$_2^+$ exist as the octahedrally coordinated cation VO$^{2+}\cdot$5H$_2$O [14] and the mononuclear aquadioxo cation VO$_2^+\cdot$4H$_2$O [15,16], respectively. It is also reported that dinuclear oxovanadium (IV, V) species containing the [V$_2$O$_3$]$^{3+}$core can be easily formed from the mixtures of the constituents VO^{2+} (aq) and VO$_2^+$ (aq) ions because of their favorable thermodynamic stability [17–20]. However, the dinuclear oxovanadium (IV, V) complex formed shows the kinetic lability due to the weak interaction between the VO^{2+} (aq) and VO$_2^+$

(aq) ions, and thus the species VO^{2+} (aq) and VO$_2^+$ (aq) are only slightly consumed during the reaction [17]. Thus, the formation of the oxovanadium (IV, V) complex is out of the consideration here for simplicity. Thereby, based on the experimental values of $m_{VO^{2+}}$, m_{H^+} and n, a new CEC mechanism involving two intermediates HV$_2$O$_3^{3+}\cdot$9H$_2$O and HVO$_2^{2+}\cdot$4H$_2$O is proposed as follows:

$$2\left[VO^{2+}\cdot5H_2O\right] \underset{k_{-23}}{\overset{k_{23}}{\rightleftharpoons}} HV_2O_3^{3+}\cdot9H_2O + H^+ \quad (25)$$

$$HV_2O_3^{3+}\cdot9H_2O \underset{k_{-24}}{\overset{k_{24}}{\rightleftharpoons}} HVO_2^{2+}\cdot4H_2O + VO^{2+}\cdot5H_2O + e \quad (26)$$

$$HVO_2^{2+}\cdot4H_2O \underset{k_{-25}}{\overset{k_{25}}{\rightleftharpoons}} VO_2^+\cdot4H_2O + H^+ \quad (27)$$
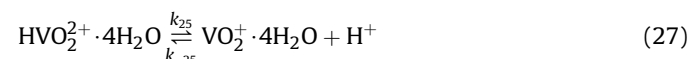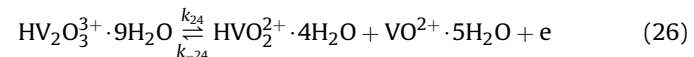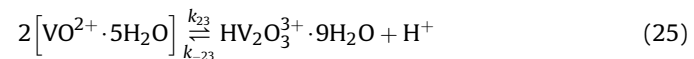
Because the dinuclear mixed-valence oxidovanadium (IV, V) complex is considered to have almost a linear V−O−V bridge with the terminal oxo groups in mutually transpositions shown as

$$\overset{O}{\overset{\|}{V}}-O-\overset{}{\underset{\|}{\underset{O}{V}}}$$ [17–19], the intermediates HV$_2$O$_3^{3+}\cdot$9H$_2$O and

HVO$_2^{2+}\cdot$4H$_2$O probably have the structural forms of $[\overset{O}{\overset{\|}{V}\text{-O-V}}]^{3+}\cdot$9H$_2$O

$$\underset{OH}{|}$$

Fig. 6. The shift of I_d at the potential of 1.4 V with $\omega^{1/2}$.
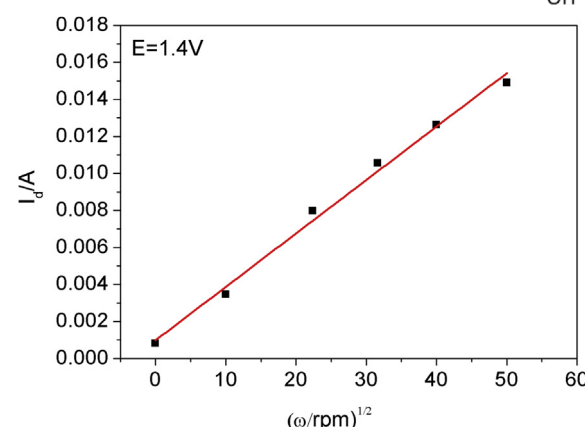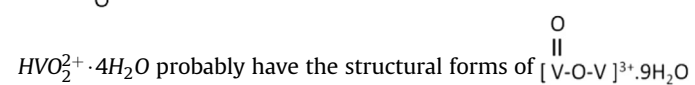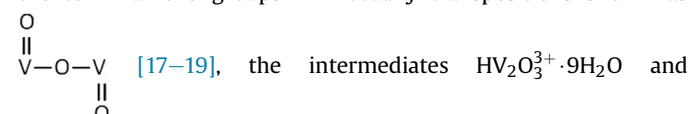
Table 4
The reaction order of H$^+$ on the glassy carbon electrode during the oxidation reaction of VO^{2+}.

E/V	0.68 V	0.69 V	0.7 V	0.71 V	0.72 V	Mean value of m_{H^+}
m_{H^+}	-0.91	-0.90	-0.89	-0.87	-0.85	-0.89
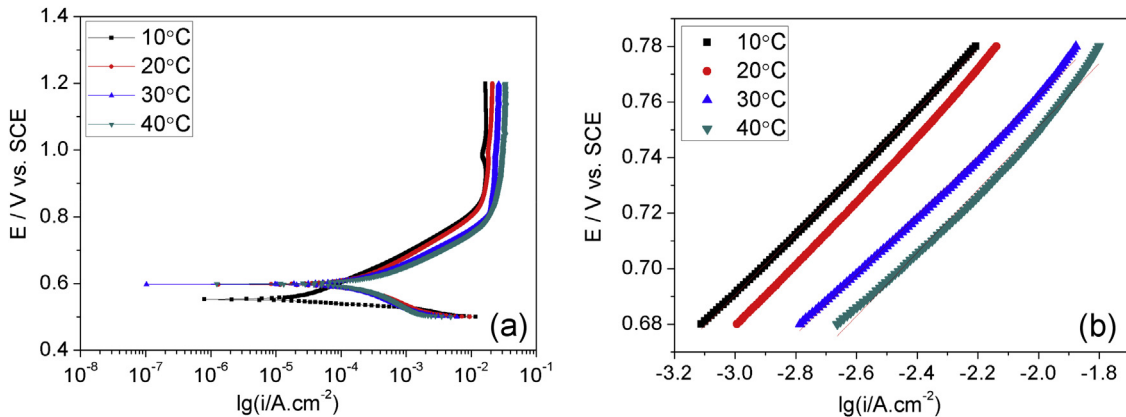
Fig. 7. Polarization curves (a) and the shift of E vs. lg$i$ (b) at various temperatures on the spectroscopically pure graphite electrode with the sweep rate of 0.5 mV s^{-1} in 1.0 M VOSO$_4$ + 0.5 M H$_2$SO$_4$ static solution.

and $\begin{matrix}[O{=}V]^{2+} \\ | \\ OH\end{matrix}$. 4H$_2$O, respectively, which, however, have not been investigated experimentally in the present study.

The theoretical values of $m_{VO^{2+}}$ and m_{H^+} for the oxidation of VO^{2+} based on the reactions (25)–(27) are similarly calculated as the above.

Firstly, if step (25) is rate determining, the reaction current density is given by:

$$i = Fk_{23}\left[VO^{2+}\right]^2 \qquad (28)$$

From eq. (28) the values of $m_{VO^{2+}}$ and m_{H^+} are calculated to be 2 and 0, respectively.

Next, in case step (26) is rate determining and the other steps are approximately at equilibrium, the reaction current density is expressed by:

$$i = Fk_{24}\left[HV_2O_3^{3+}\right]\exp\left[\frac{\beta}{RT}FE\right] \qquad (29)$$

For step (25) at equilibrium, the following expression can be obtained:

$$k_{23}\left[VO^{2+}\right]^2 = k_{-23}\left[H^+\right]\left[HV_2O_3^{3+}\right] \qquad (30)$$

Introducing eq. (30) into eq. (29), eq. (29) is changed to:

$$i = Fk_{24}\frac{k_{23}\left[VO^{2+}\right]^2}{k_{-23}\left[H^+\right]}\exp\left[\frac{\beta}{RT}FE\right] \qquad (31)$$

From eq. (31) the values of $m_{VO^{2+}}$ and m_{H^+} can be estimated to be 2 and −1, respectively.

Finally, if step (27) is rate determining, the steps (25) and (26) can be thought to be at equilibrium. Then, the reaction current density is illustrated by:

$$i = Fk_{25}\left[HVO_2^{2+}\right] \qquad (32)$$

The same reaction rate in the forward and reverse directions for both the steps (25) and (26) can be described as:

$$Fk_{24}\left[HV_2O_3^{3+}\right]\exp\left[\frac{\beta}{RT}FE\right] = Fk_{-24}\left[HVO_2^{2+}\right]$$
$$\times \left[VO^{2+}\right]\exp\left[\frac{-(1-\beta)}{RT}FE\right] \qquad (33)$$

$$k_{23}\left[VO^{2+}\right]^2 = k_{-23}\left[H^+\right]\left[HV_2O_3^{3+}\right] \qquad (34)$$

Thus, according to eqs. (32)–(34), the reaction current density can be given by:

$$i = F\frac{k_{25}k_{24}k_{23}}{k_{-24}k_{-23}}\frac{\left[VO^{2+}\right]}{\left[H^+\right]}\exp\left[\frac{FE}{RT}\right] \qquad (35)$$

It can be estimated from eq. (35) that the values of $m_{VO^{2+}}$ and m_{H^+} are 1 and −1, respectively.

The above calculations indicate that when the step (26) (E step) is rate determining, the theoretical values of $m_{VO^{2+}}$ and m_{H^+} comply well with the experimental results. Thereby, it is reasonable to consider that the oxidation reaction of VO^{2+} may follow the new CEC mechanism with an electrochemical reaction as the rate-limited process. In contrast with the mechanisms proposed by Gattrel et al. [6,7], the new CEC mechanism involves a possible combination between VO^{2+} ions during the oxidation reaction of VO^{2+}. Moreover, the reaction orders of VO^{2+} and H$^+$ for the oxidation reaction of VO^{2+} are 2 and −1, respectively. In this case, the reaction current density of VO^{2+} shown in eq. (31) can be also presented by

Table 6
The formal potential ($E^{O'}$) and the rate constants of the vanadium redox reaction (k_s) at different temperatures calculated from the cyclic voltammograms for the VO$_2^+$/ VO^{2+} redox reaction on the spectroscopically pure graphite electrode.

$T/^\circ$C	$E^{O'}/$V	$k_s/(10^{-3}$ cm s$^{-1})$
10	0.940	1.91
20	0.940	2.13
30	0.935	3.26
40	0.945	5.03
50	0.935	5.11

Table 5
The charge transfer coefficients (β) on the spectroscopically pure graphite electrode at various temperatures.

| $T/^\circ$C		10	20	30	40	Mean value
Tafel slope (0.68−0.78 V)/(V dec^{-1})		0.111	0.116	0.107	0.114	
β			0.531	0.509	0.551	0.518	0.53
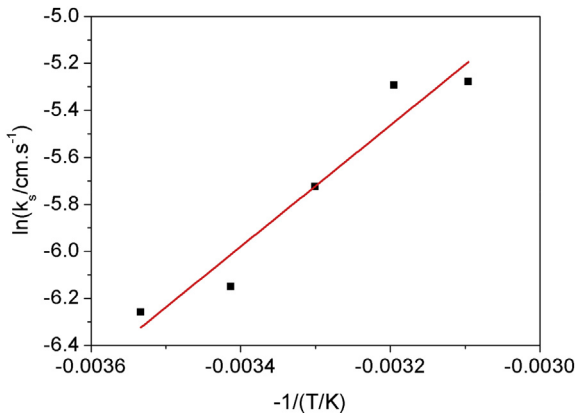
Fig. 8. The shift of $\ln k_s$ with $-1/T$ at various temperatures.

$$i = Fk\frac{[\text{VO}^{2+}]^2}{[\text{H}^+]}\exp\left[\frac{\beta}{RT}FE\right] \tag{36}$$

where k is the reaction rate constant. When the electrochemical reaction rate constant at standard state (k_s) is taken as a substitute for k, eq. (36) can be described as [12]:

$$i = Fk_s\frac{[\text{VO}^{2+}]^2}{[\text{H}^+]}\exp\left[\frac{\beta}{RT}F\left(E-E^{o'}\right)\right] \tag{37}$$

where $E^{O'}$ is the formal potential of the $\text{VO}^{2+}/\text{VO}_2^+$ redox reaction.

3.5. An oxidation reaction kinetic equation of VO^{2+} on the spectroscopically pure graphite electrode

The above results indicate that the proposed CEC model with the electrochemical reaction as the rate-limiting step is reasonable to be used to describe the oxidation reaction of VO^{2+}. To establish the real reaction kinetics of VO^{2+}, some parameters shown in eq. (37) should be known. Fig. 7a shows the polarization curves at various temperatures on the spectroscopically pure graphite electrode in 1.0 M VOSO_4 + 0.5 M H_2SO_4 static solutions. Fig. 7b presents the corresponding plots of E vs. $\lg i$ with the slope as Tafel slope ($\partial E/\partial \lg i$). Furthermore, the parameter β in eq. (37) can be defined as the following equation [12]:

$$\frac{\partial E}{\partial \lg i} = \frac{2.303RT}{\beta nF} \tag{38}$$

Thus, the values of Tafel slope and β at different temperatures can be obtained, as listed in Table 5. The mean value of β is obtained to be 0.53.

With the cyclic voltammograms on the spectroscopically pure graphite electrode in 1.2 M VOSO_4 + 3.0 M H_2SO_4 static solutions at various temperatures examined, the formal potential ($E^{O'}$) and the rate constants of the vanadium redox reaction at standard state (k_s) at various temperatures are estimated, as listed in Table 6, and the corresponding calculations have been shown in detail in another unpublished paper submitted. The mean value of $E^{O'}$ is 0.94 V. Based on Table 6, the change of $\ln k_s$ with $-1/T$ is obtained, as shown in Fig. 8. The reaction rate constant k_s at standard state can be given by the Arrhenius equation [12]:

$$k_s = A_0 \exp\left(-\frac{\Delta G^\theta}{RT}\right) \tag{39}$$

where ΔG^θ is the reaction activation energy at standard state, A_0 the temperature-independent factor. Thus, from Fig. 8, the values of ΔG^θ and A_0 can be estimated as 21.774 kJ mol^{-1} and 18.202 cm s^{-1}, respectively. Introducing the values of these parameters into eq. (37), the kinetic equation for the oxidation reaction of VO^{2+} on the spectroscopically pure graphite electrode can be given as:

$$i = 1.756 \times 10^6 C_{\text{VO}^{2+}}^2 C_{\text{H}^+}^{-1} \exp\left(-\frac{69820}{RT}\right)\exp\left(\frac{0.53FE}{RT}\right) \tag{40}$$

where E is the electrode potential versus SCE, i is the anodic current density (A cm^{-2}), $C_{\text{VO}^{2+}}$ and C_{H^+} are the bulk concentrations of VO^{2+} and H^+ ions in the electrolyte solutions (mol cm^{-3}), respectively.

According to the kinetic eq. (40), the change of $\lg i$ with E can be obtained. Fig. 9a presents a comparison between the theoretical and experimental polarization curves at 10 °C in 1.0 M VOSO_4 + 0.5 M H_2SO_4 static solution. It can be seen that, except for the potentials higher than 0.78 V, the real kinetic equation fits the experimental data quite well. Since the kinetic equation is just usable at the potentials where the electrochemical polarization is rate determining, these are the very expected results. Similar results have also been obtained at 25 °C in 1.5 M VOSO_4 + 3.0 M H_2SO_4 static solution, as shown in Fig. 9b, respectively. Therefore, the kinetic equation of eq. (40) can be
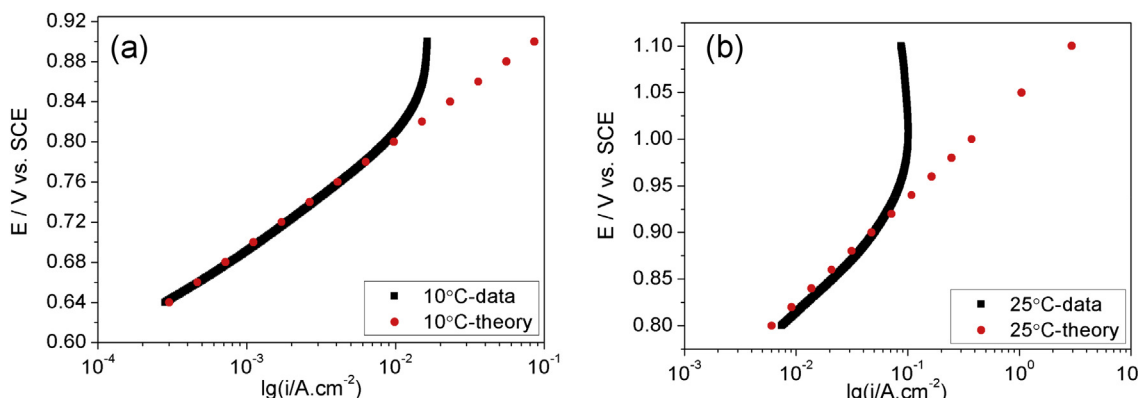

Fig. 9. The kinetic equation fitted to a set of polarization plots on the spectroscopically pure graphite electrode in 1.0 M VOSO_4 + 0.5 M H_2SO_4 static solution at 10 °C (a) and 1.5 M VOSO_4 + 3.0 M H_2SO_4 static solution at 25 °C (b).

well used to predict the polarization behavior of the spectroscopically pure graphite electrode over a range of temperatures and concentrations in V (IV) acidic solutions.

4. Conclusions

The oxidation reaction mechanism of VO^{2+} on a rotating disk electrode such as basal plane pyrolytic graphite (GB) and glassy carbon (GC) disk electrodes has been examined by potentiodynamic polarization in sulfuric acid solutions with various pH and vanadium concentrations, respectively. Based on the polarization results, the reaction orders of VO^{2+} ($m_{VO^{2+}}$) and H^+ (m_{H^+}) for the oxidation reaction of VO^{2+} on carbon electrodes have been calculated to be 2 and -1, respectively, which are inconsistent with the theoretical results based on the possible reaction mechanisms including chemical (C)-chemical (C)-electrochemical (E), ECC and CEC mechanism available in the literature. The electron transfer number (n) of the oxidation reaction of VO^{2+} is calculated to be approximately 1. Based on the experimental values of $m_{VO^{2+}}$, m_{H^+} and n, a new CEC oxidation reaction mechanism shown in eqs. (23)–(25) is thus proposed to represent the oxidation of VO^{2+}. The theoretic reaction orders of VO^{2+} and H^+ based on the new mechanism are in good accord with the experimental results when the electrochemical polarization is rate determining. Furthermore, a corresponding kinetic equation has been built up for the oxidation reaction of VO^{2+} on a spectroscopically pure graphite electrode as shown in eq. (40), and can be well used to predict the polarization behavior over a range of temperatures and concentrations in V(IV) acidic solutions. Though the new reaction model can be well applied to a certain extent, more extensive studies are still required to understand the new mechanism, including the oxidation reaction on different carbon electrodes, the reaction intermediates involved, etc.

References

[1] C. Ding, H. Zhang, X. Li, T. Liu, F. Xing, J. Phys. Chem. Lett. 4 (2013) 1281–1294.
[2] M. Skyllas-Kazacos, M.H. Chakrabarti, S.A. Hajimolana, F.S. Mjalli, M. Saleem, J. Electrochem. Soc. 158 (2011) R55–R79.
[3] W. Wang, Q. Luo, B. Li, X. Wei, L. Li, Z. Yang, Adv. Funct. Mater. 23 (2012) 970–986.
[4] E. Sum, M. Skyllas-Kazacos, J. Power Sources 15 (1985) 179–190.
[5] E. Sum, M. Rychcik, M. Skyllas-Kazacos, J. Power Sources 16 (1985) 85–95.
[6] M. Gattrell, J. Park, B. MacDougall, J. Apte, S. McCarthy, C.W. Wu, J. Electrochem. Soc. 151 (2004) A123–A130.
[7] M. Gattrell, J. Qian, C. Stewart, P. Graham, B. MacDougall, Electrochim. Acta 51 (2005) 395–407.
[8] D. Aaron, Z. Tang, A.B. Papandrew, T.A. Zawodzinski, J. Appl. Electrochem. 41 (2011) 1175–1182.
[9] C.N. Sun, F.M. Delnick, D.S. Aaron, A.B. Papandrew, M.M. Mench, T.A. Zawodzinski, ECS Electrochem. Lett. 2 (2013) A43–A45.
[10] D. Aaron, C.N. Sun, M. Bright, A.B. Papandrew, M.M. Mench, T.A. Zawodzinski, ECS Electrochem. Lett. 2 (2013) A29–A31.
[11] G. Oriji, Y. Katayama, T. Miura, J. Power Sources 139 (2005) 321–324.
[12] H.L. Hu, N. Li, Electrochemical Measurements, National Defense Industry Press, Beijing, 2011, pp. 96–107, 18–21.
[13] Q.X. Zha, et al., An Introduction to Electrode Process Kinetics, third ed., Science Press, Beijing, 2002, pp. 202–208.
[14] G. Oriji, Y. Katayama, T. Miura, Electrochim. Acta 49 (2004) 3091–3095.
[15] J.J. Cruywagen, J.B.B. Heyns, A.N. Westra, Inorg. Chem. 35 (1996) 1556–1559.
[16] N. Kausar, R. Howe, M. Skyllas-Kazacos, J. Appl. Electrochem. 31 (2001) 1327–1332.
[17] P. Blanc, C. Madic, J.P. Launay, Inorg. Chem. 21 (1982) 2923–2928.
[18] M. Mahroof-Tahir, A.D. Keramidas, R.B. Goldfarb, O.P. Anderson, M.M. Miller, D.C. Crans, Inorg. Chem. 36 (1997) 1657–1668.
[19] S.K. Dutta, S. Samanta, S.B. Kumar, O.H. Han, P. Burckel, A.A. Pinkerton, M. Chaudhur, Inorg. Chem. 38 (1999) 1982–1988.
[20] K. Bhattacharya, M. Maity, S.M.T. Abtab, M.C. Majee, M. Chaudhury, Inorg. Chem. 52 (2013) 9597–9605.